

Supporting Information

**Development and Application of a Digestion-Raman Analysis Approach for Studying
Multiwall Carbon Nanotube Uptake in Lettuce**

Kamol K Das¹, Yaqi You^{1*}, Miguel Torres², Felipe Barrios-Masias², Xilong Wang³, Shu Tao³,
Baoshan Xing⁴, and Yu Yang^{1*}

¹Department of Civil and Environmental Engineering, University of Nevada Reno, MS258,
1664 N. Virginia Street, Reno, Nevada 89557, USA;

²Department of Agriculture, Nutrition & Veterinary Science, University of Nevada Reno,
MS202, 1664 N. Virginia Street, Reno, Nevada 89557, USA;

³Laboratory for Earth Surface Processes, College of Urban and Environmental Sciences, Peking
University, Beijing 100871, China;

⁴Stockbridge School of Agriculture, University of Massachusetts Amherst, 410 Paige
Laboratory, Amherst, MA 01003, USA.

*For correspondence, please email yuy@unr.edu or you.yaqi@gmail.com.

SUPPLEMENTARY MATERIALS AND METHODS

Transmission electron microscopy (TEM) analysis

TEM was used to confirm the presence of multiwall carbon nanotubes (MWCNTs) in the spiked plant tissues as well as in the lettuce plants grown hydroponically with MWCNTs. Spiked plant tissues used in the approach development step were digested with HNO₃, washed with Milli-Q water for three times, and collected and re-suspended in 100% ethanol. An aliquot (30 µL) of each sample was loaded on a holey carbon-coated copper grid (400 mesh, Pacific-Grid Tech) and dried at room temperature. Grids were observed under a TEM (JEOL 2100F operating at 200 kV), and electron diffraction was recorded for the area under beam line as an indicator of crystalline MWCNTs.

For lettuce grown in hydroponic systems, the harvested plants were thoroughly rinsed with autoclaved Milli-Q water to remove particles attached on the root surface and oven-dried at 80 °C overnight. Dried plants were dissected aseptically into three parts of root, stem, and leaf. The root and leaf samples were further dissected into 1-2 mm³ pieces and fixed with Karnovsky's fixative.¹ Fixed samples were stored at 4 °C before processed using an establish protocol at the Electron Microscopy Laboratory, Department of Cell Biology and Human Anatomy, University of California at Davis.² Briefly, samples were rinsed with 100 mM sodium phosphate buffer for several times, post-fixed in sodium phosphate buffered 1% osmium tetroxide for 2 hours, rinsed with autoclaved Milli-Q water, and incubated in 0.1% tannic acid for 30 min. After a brief rinse with autoclaved Milli-Q water, samples were stained with 1% uranyl acetate for 90 min, followed by slow dehydration through a series of graded acetone, and embedded in an epoxy resin mixture through complete infiltration overnight. The resulting blocks were cut into thin sections using a Leica Ultracut UCT ultramicrotome (Solms, Germany)

and diamond knives (DiATOME, Switzerland). Thin sections were placed on grids, post stained with 4% uranyl acetate and citrate, and then observed under a Philips CM120 Biotwin TEM (FEI Company, Oregon, USA).

SUPPLEMENTARY RESULTS AND DISCUSSION

Uptake and translocation of MWCNTs in lettuce plants

Effects of MWCNTs on the growth and physiology of lettuce

After 18 days, exposure to 5 or 10 mg/L pristine MWCNT (p-MWCNT) enhanced cumulative transpiration of water in lettuce plants by 5.83% or 8.36%, respectively, as compared to the non-exposure condition ($p>0.4$, Mann-Whitney U test) (Figure 4-A). In contrast, exposure to 20 mg/L p-MWCNT inhibited cumulative transpiration by 9.51% ($p>0.1$, Mann-Whitney U test). Meanwhile, exposure to 5 mg/L or 10 mg/L carboxyl-functionalized (c-MWCNT) decreased cumulative transpiration by 3.03% ($p>0.8$, Mann-Whitney U test) or 14.22% ($p=0.063$, Mann-Whitney U test), respectively, whereas 20 mg/L c-MWCNT resulted in a 4.55% increase in cumulative transpiration ($p>0.6$, Mann-Whitney U test). Most of the exposed plants had less dry biomass than the controls, but the difference was not significant in most cases ($p>0.3$ in Mann-Whitney U test) (Figure S9). Among all the plants, those exposed to 10 mg/L c-MWCNT had the lowest dry biomass, significantly less than control plants without exposure ($p<0.03$ in Mann-Whitney U test).

Exposure to MWCNTs greatly affected root system development in lettuce plants (Figure S10). In particular, root length of the exposed lettuce plants followed the same trend as their cumulative transpiration (Figure S11). Compared to control plants, exposure to 5 or 10 mg/L p-

MWCNT resulted in longer roots whereas exposure to 20 mg/L p-MWCNT led to much shorter roots; exposure to 5 or 20 mg/L c-MWCNT yielded longer roots while exposure to 10 mg/L c-MWCNT generated shorter roots. However, these effects were not significant ($p>0.6$ in Mann-Whitney U test). Regardless of their types and concentrations, MWCNTs induced the development of lateral roots in lettuce plants (Figure 4-B1). Such an effect was significant for the 10 mg/L c-MWCNT treatment ($p<0.03$ in Mann-Whitney U test). In addition to their impacts on the root system, both MWCNTs resulted in increased leaf membrane leakage at most doses, and this effect was significant for 10 mg/L c-MWCNT (1.49 times higher than the controls, $p<0.03$ in Mann-Whitney U test) (Figure 4-B2). For p-MWCNT, the severest leaf cell damage was observed in plants exposed to 5 mg/L p-MWCNT (82.7% higher than control plants, $p>0.4$ in Mann-Whitney U test).

Effects of MWCNTs on diverse plant species at various development stages have been documented and complex plant physiological responses have been reported.³⁻⁶ Depending on plant species and CNT properties such as size, surface functionality, impurities, and aggregation states, both stimulation and inhibition effects have been observed. In one study, MWCNTs were found to stimulate cumulative water transpiration and enhance dry biomass in maize, in a charge-dependent way such that negatively charged MWCNT displayed a stronger stimulation effect than pristine MWCNT or positively charged MWCNT at the same concentration.⁷ The same study also found MWCNTs to inhibit transpiration and reduce dry biomass in soybean, with negatively charged MWCNT showing the least effect. Enhanced root growth has been seen in rice, radish, rape, ryegrass, lettuce, corn, and cucumber.⁸ A dual pattern of MWCNT's impacts on several plant species was also reported, such that lower concentrations increased plant fresh weight and root length whereas higher concentrations reduced biomass and root length, with leaf

cell damage occurring at all the concentrations.⁹ However, another study reported no influence of MWCNTs at 2000 mg/L on lettuce root length.¹⁰ More research is needed to address mechanisms underlying MWCNT-induced physiological changes in plants, and a more comprehensive understanding of impacts of CNTs on plants in general is necessary for the sustainable development of nanotechnology in agriculture.

Concentration-dependent detection of MWCNTs

We examined the possibility of quantifying MWCNTs in spiked lettuce leaves based on the G-band and D-band intensities. A preliminary linear correlation between p-MWCNT concentrations and G-band or D-band intensities was observed, although there were larger variations for lower concentrations (Figure S8). No correlation was observed for c-MWCNT. The lack of linear correlation for c-MWCNT was likely due to covalent bindings of a variety of biomolecules (e.g., sugar moieties, oligonucleotides, peptide nucleic acids, and proteins) to carboxylic groups on c-MWCNT's surface,¹¹ which substantially influenced the intensity of G-band and D-band of c-MWCNT at lower concentrations (Figure S8).

Detection of MWCNT uptake and translocation in lettuce

Based on the preliminary linear correlation between p-MWCNT concentrations and G-band intensities, we estimated p-MWCNT concentrations to be 15–220 mg/kg dry weight in the plants exposed to 5–20 mg/L p-MWCNT, except for leaves of the plants exposed to 20 mg/L p-MWCNT that showed no MWCNT signals.

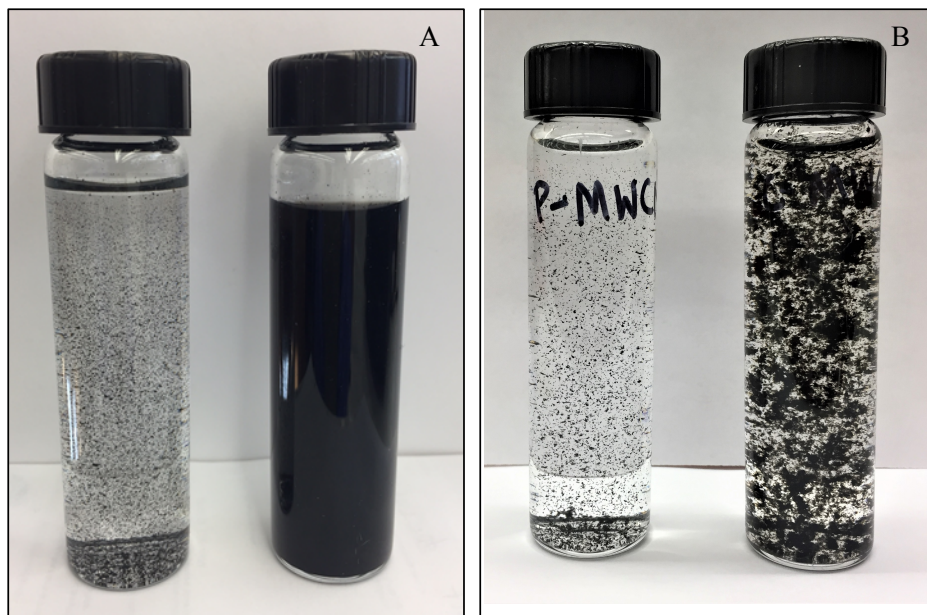


Figure S1. Dispersion of p-MWCNT (left) and c-MWCNT (right) in (A) Milli-Q water and (B) 10% Hoagland solution.

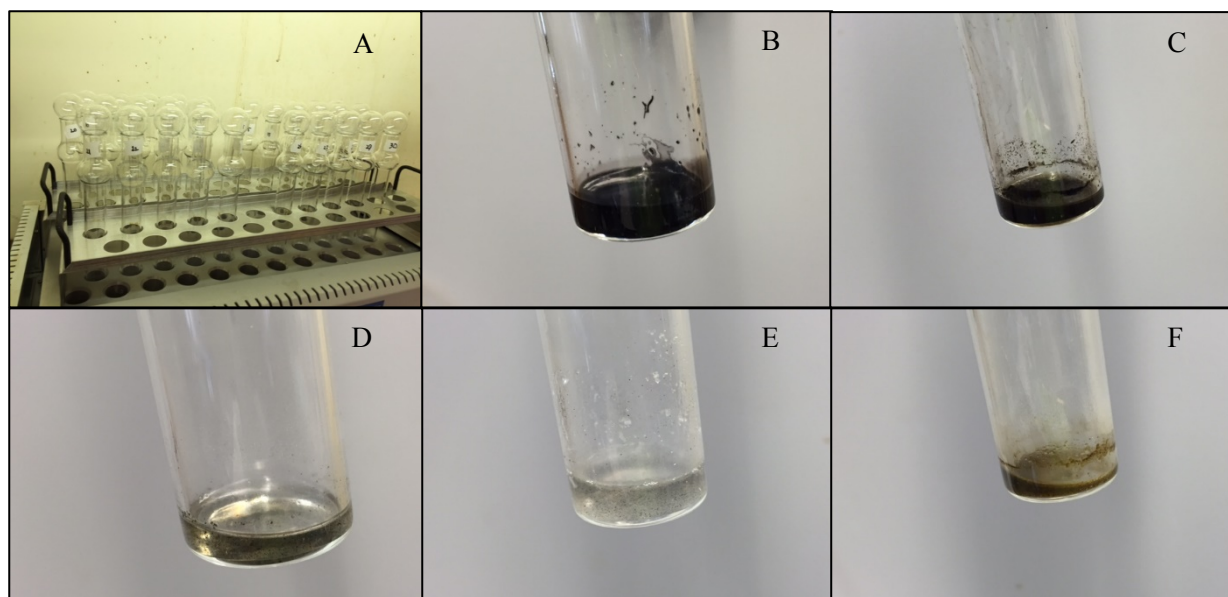


Figure S2. The digestion system used in this study (A). Residues of lettuce tissues that were spiked with 2500 mg/kg MWCNT and digested using H₂SO₄ (B), HCl (C), HNO₃ (D), H₂O₂ (E), or NH₄OH (F).

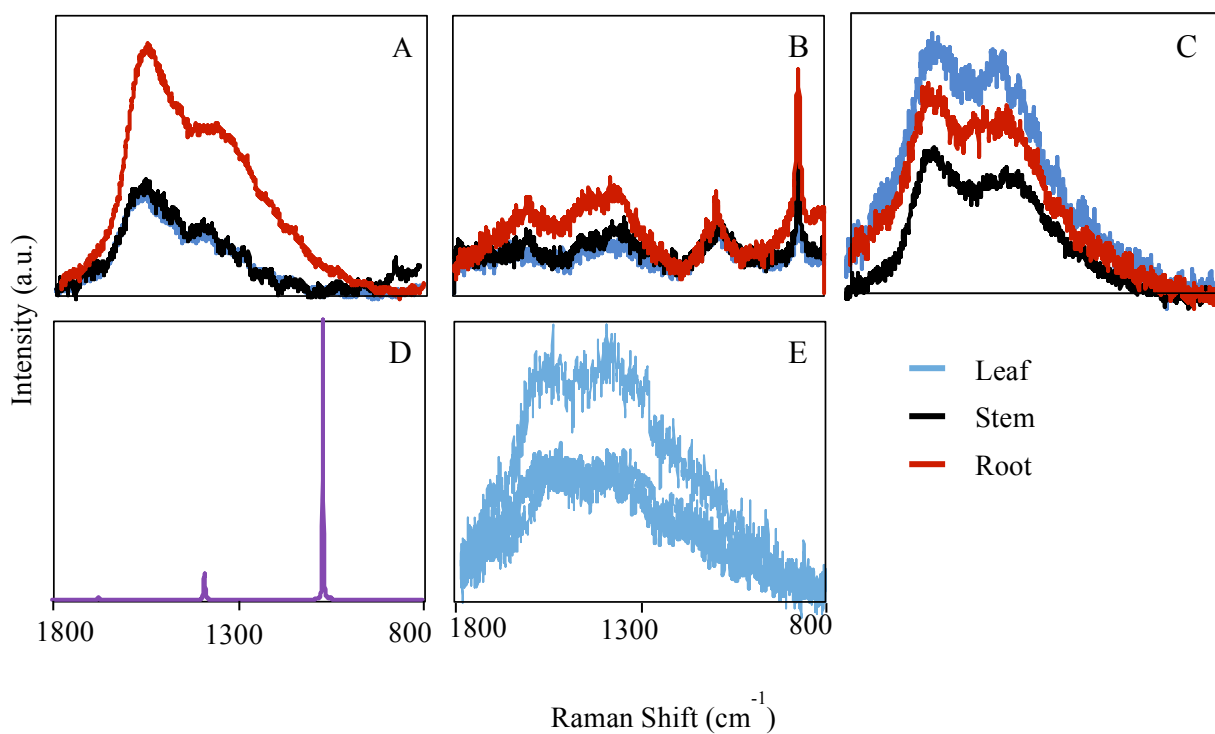


Figure S3. Raman spectra of blank leaf, stem, and root tissues digested with HCl (A), H_2O_2 (B), or NH_4OH (C), and background HNO_3 or H_2SO_4 aqueous phase (D). Each spectrum represents the average of five scans from different sample areas. The spectra of undigested leaf tissues are shown in E.

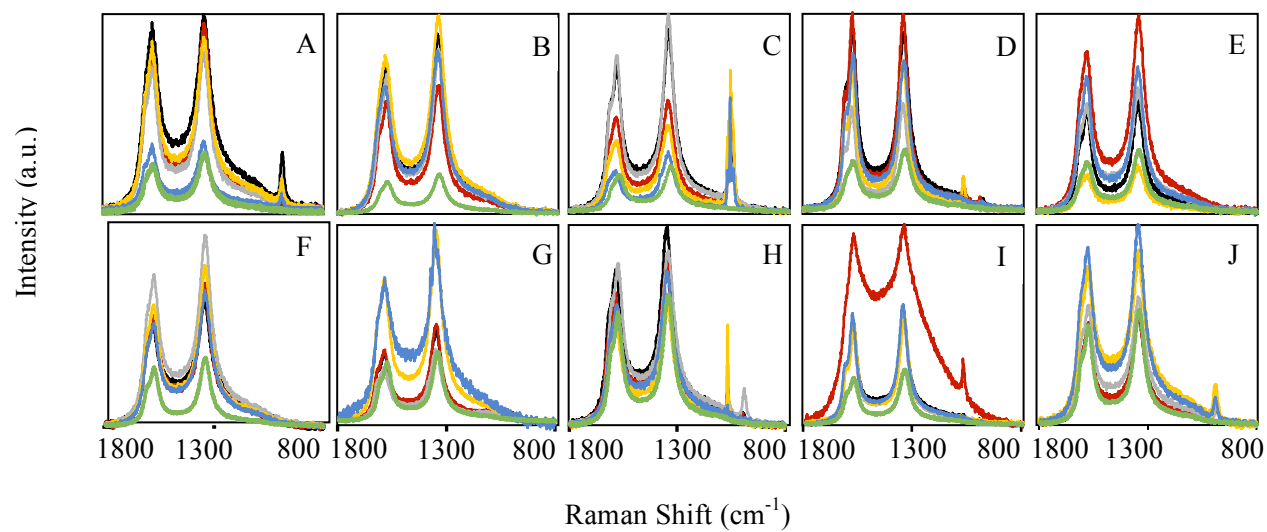


Figure S4. Raman spectra of p-MWCNT (A – E) and c-MWCNT (F – J) subjected to H₂SO₄ (A, F), HCl (B, G), HNO₃ (C, H), H₂O₂ (D, I), or NH₄OH (E, J) digestion. Green spectra represent original MWCNTs and other colors represent replicate spectra in each treatment.

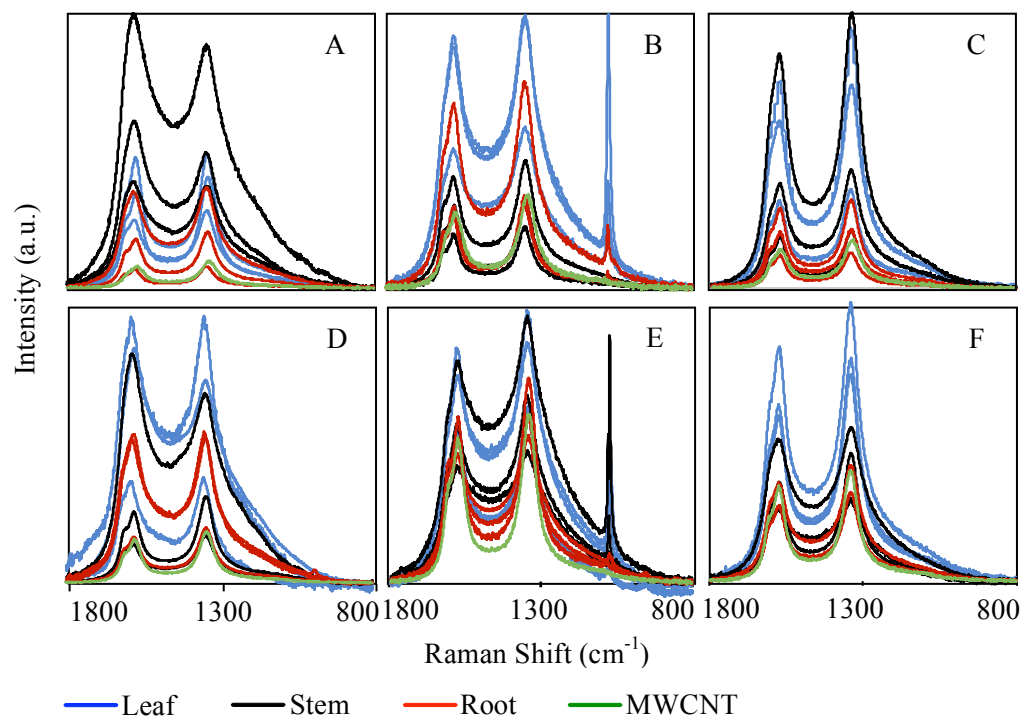


Figure S5. Raman spectra of lettuce tissues that were spiked with 2500 mg/kg p-MWCNT (A – C) or c-MWCNT (D – F) and digested with HCl (A, D), H₂O₂ (B, E), or NH₄OH (C, F). Triplicate leaf, stem, and root spectra are shown for each condition, along with pure MWCNT digested using the same reagent.

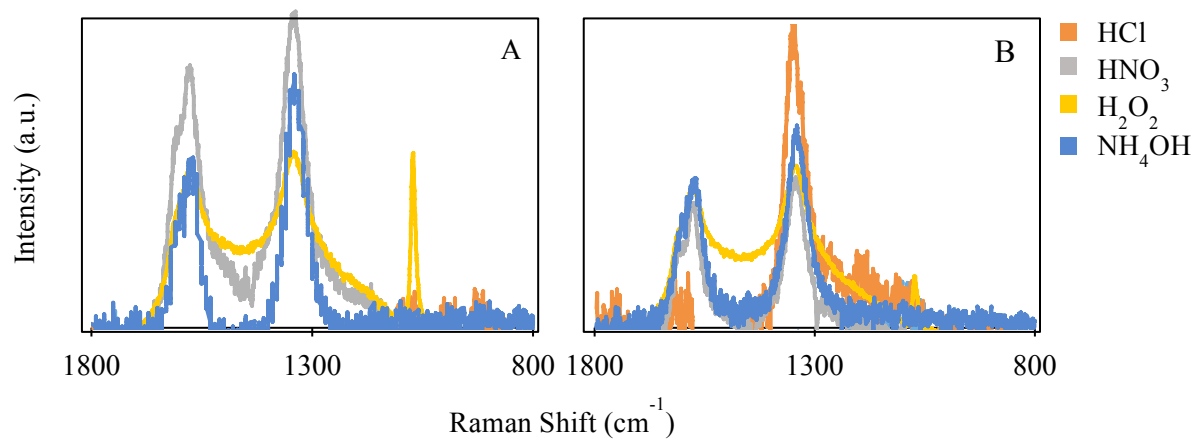


Figure S6. Raman spectra reconstructed for digestion residues of lettuce leaves spiked with 2500 mg/kg p-MWCNT (A) or c-MWCNT (B). Background signals of blank leaf tissues were subtracted from the Raman spectra of MWCNT-containing samples.

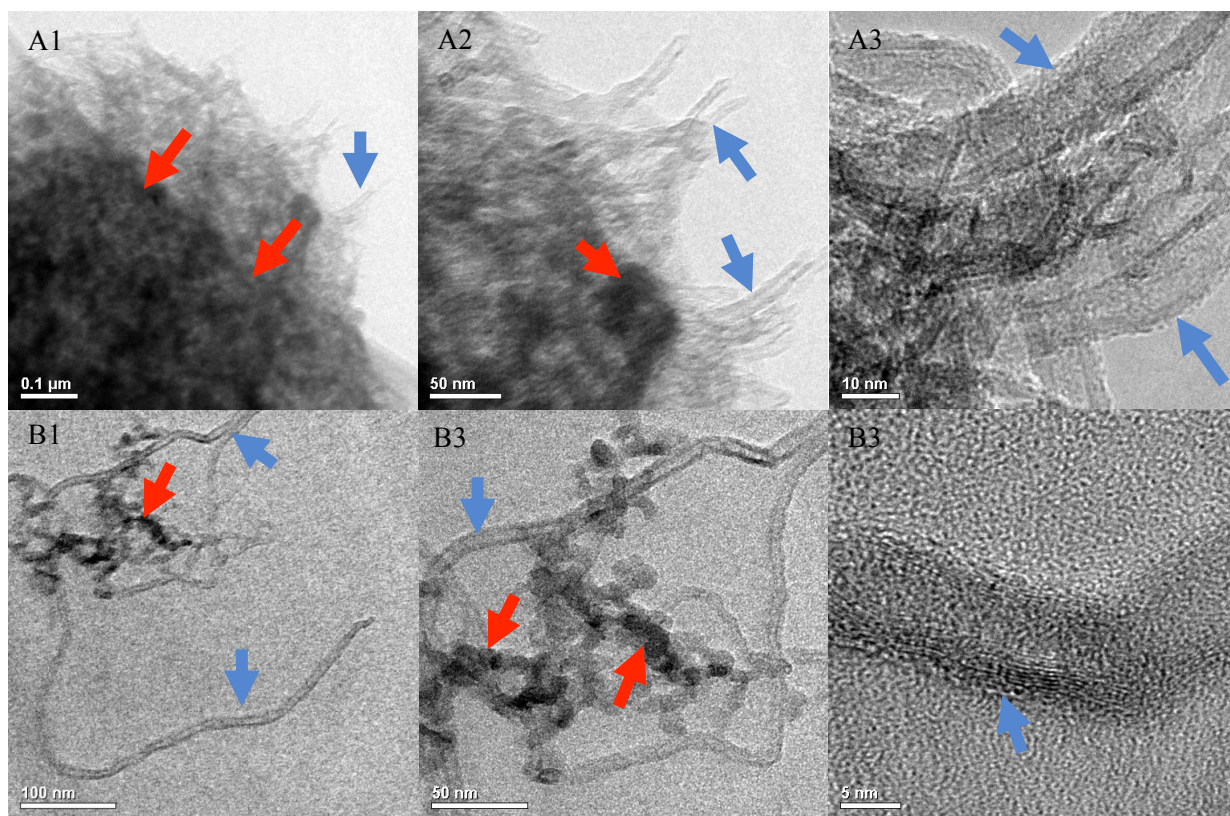


Figure S7. TEM images of HNO₃ digestion residues of leaf tissues spiked with 2500 mg/kg p-MWCNT (A1-A3) or c-MWCNT (B1-B3). The blue and red arrows indicate MWCNTs and leaf residues, respectively.

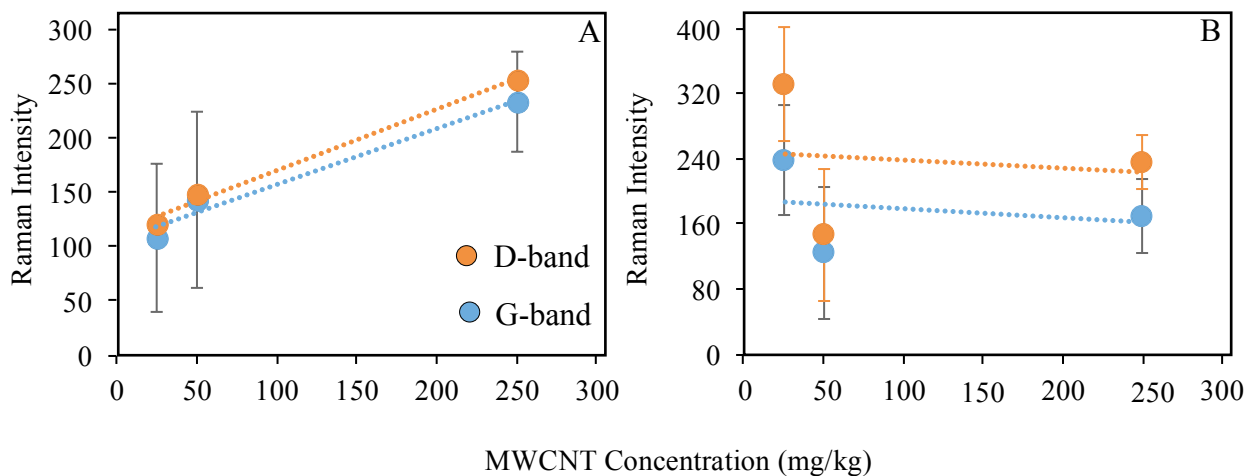
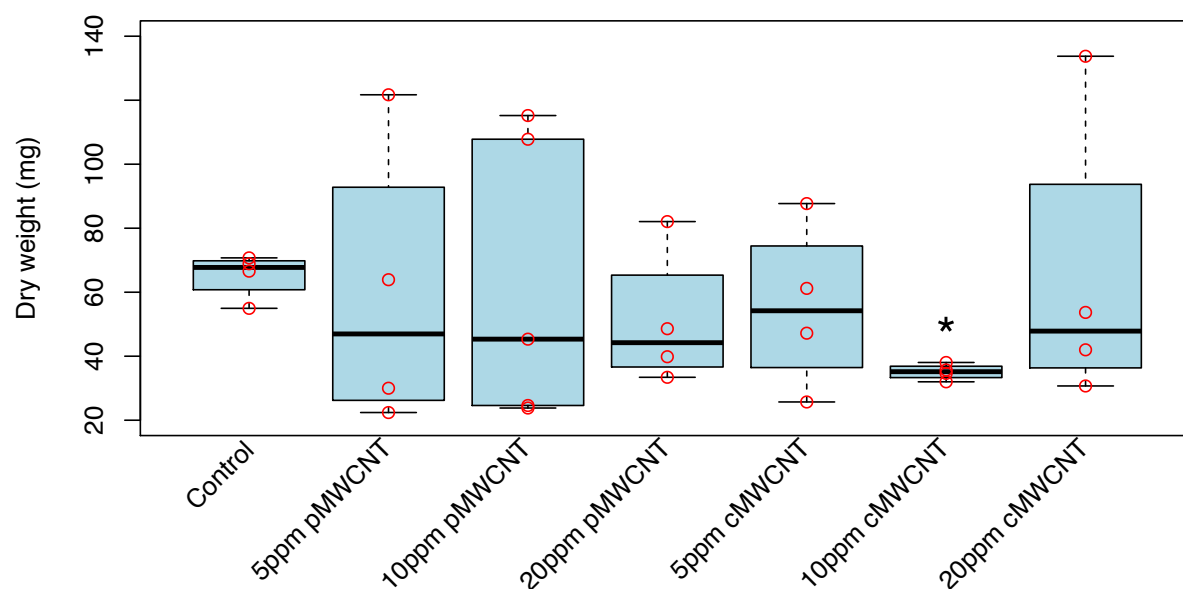


Figure S8. Correlation between the D-band or G-band intensity and the concentration of (A) p-MWCNT or (B) c-MWCNT in spiked leaf tissues. Spiked leaves were digested using HNO_3 . Data represent means and standard deviations from five independent Raman spectra. A strong linear correlation was observed for p-MWCNT, with $R^2 = 0.97$ for the D-band and $R^2 = 0.99$ for the G band. Linear correlation was not observed for c-MWCNT.

227

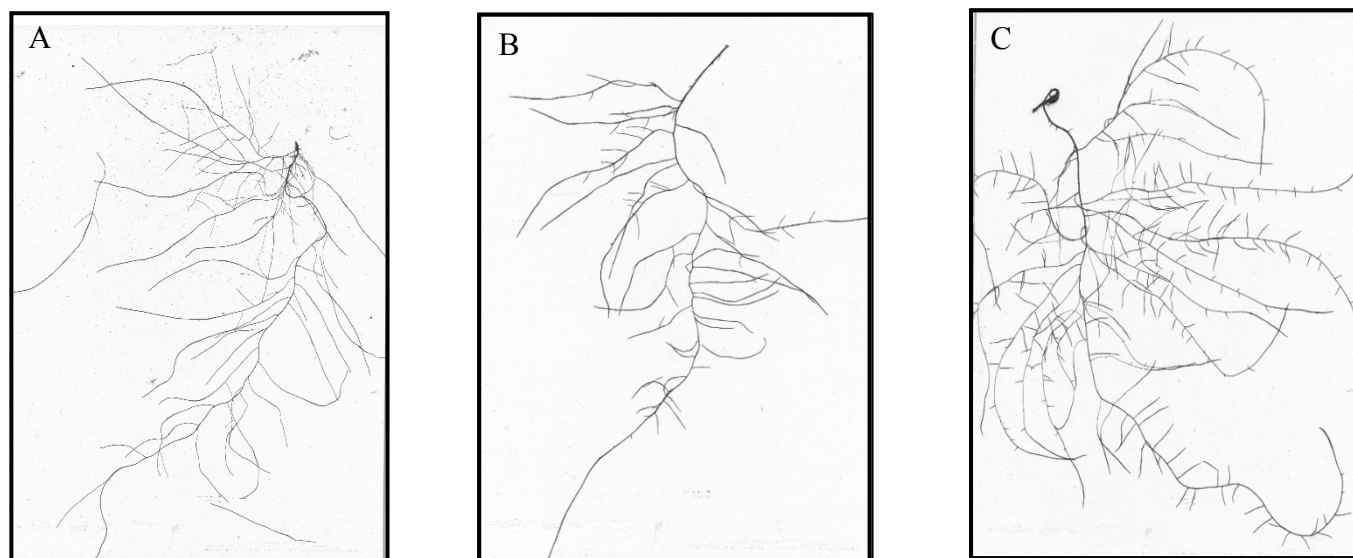


228

229 **Figure S9.** Impacts of MWCNTs on lettuce dry biomass after 18-day growth. Box-and-whisker
 230 plot shows minimum and maximum (whisker bottom and top), first and third quartile (box
 231 bottom and top), and median (line inside box) of 4–5 lettuce plants. Asterisk indicates a
 232 significant difference between exposed plants and controls.

233

234



242

243 **Figure S10.** Root systems of lettuce plants that were (A) not exposed to any MWCNT, (B)
244 exposed to 20 mg/L p-MWCNT, or (C) exposed to 20 mg/L c-MWCNT for 18 days.

245

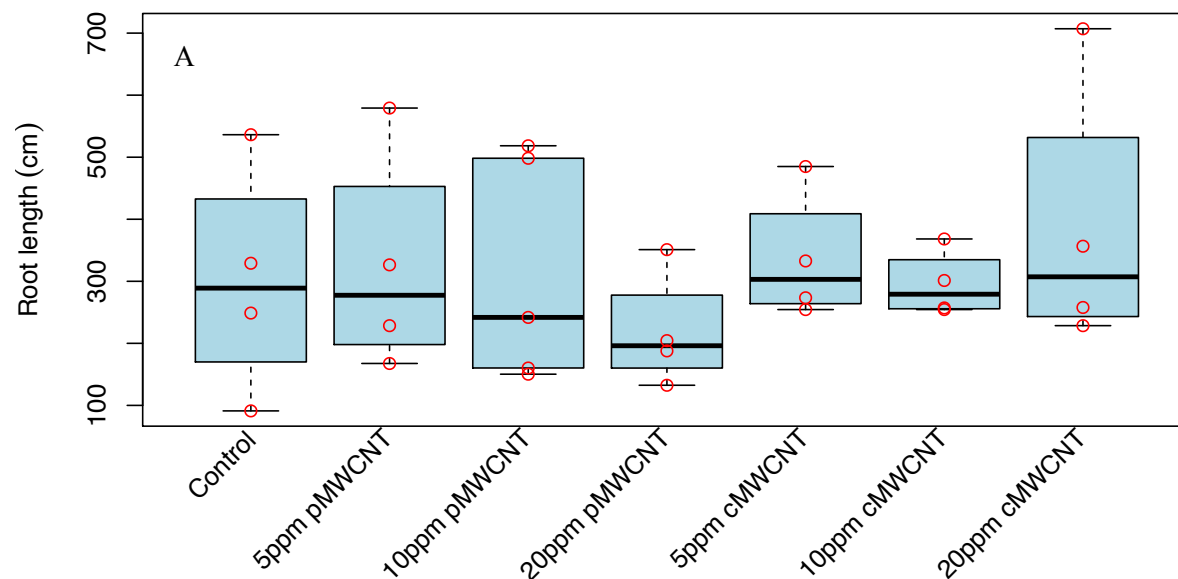


Figure S11. Impacts of MWCNTs on lettuce root length after 18-day growth. Box-and-whisker plot shows minimum and maximum (whisker bottom and top), first and third quartile (box bottom and top), and median (line inside box) of 4–5 lettuce plants.

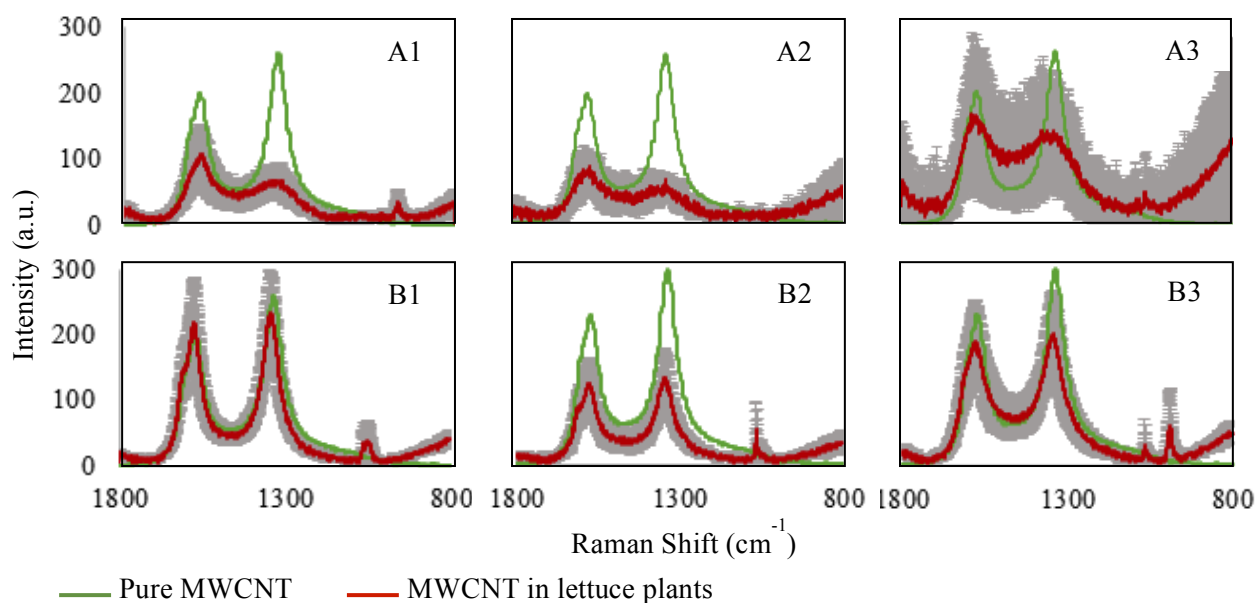


Figure S12. Raman spectra of p-MWCNT identified in the stems (A) and roots (B) of lettuce plants exposed to 5 mg/L (A1, B1), 10 mg/L (A2, B2), or 20 mg/L (A3, B3) p-MWCNT. Each spectrum of exposed plants represents the average of 6–10 sample areas, with standard deviations shown in grey.

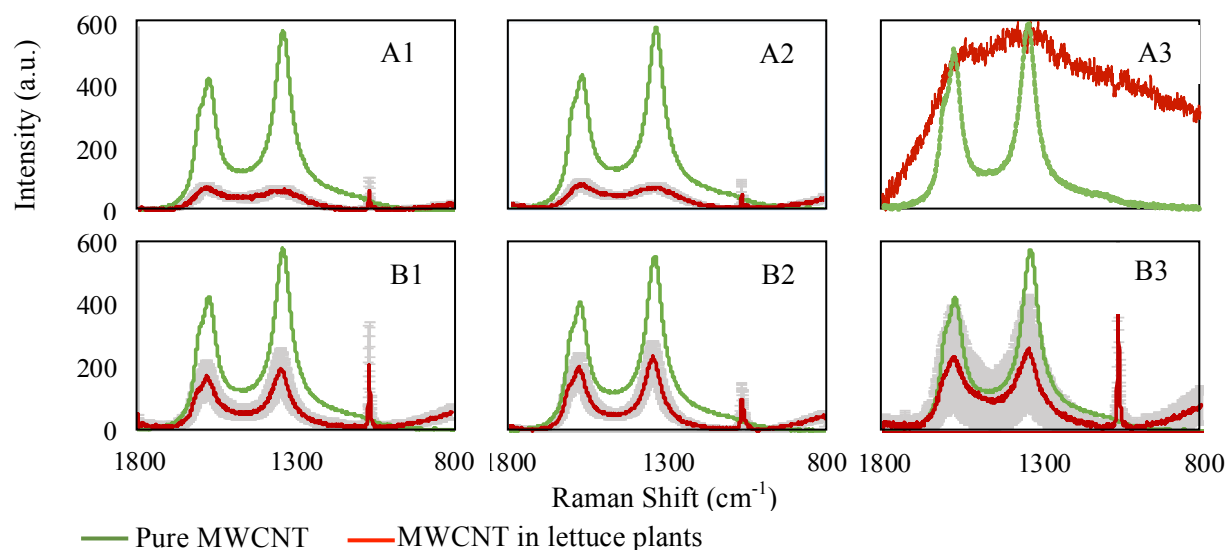


Figure S13. Raman spectra of c-MWCNT identified in the stems (A) and roots (B) of lettuce plants exposure to 5 mg/L (A1, B1), 10 mg/L (A2, B2), or 20 mg/L (A3, B3) c-MWCNT. Each spectrum of exposed plants represents the average of 6–10 sample areas, with standard deviations shown in grey. MWCNT was not detected in the stems of plants exposed to 20 mg/L c-MWCNT (A3).

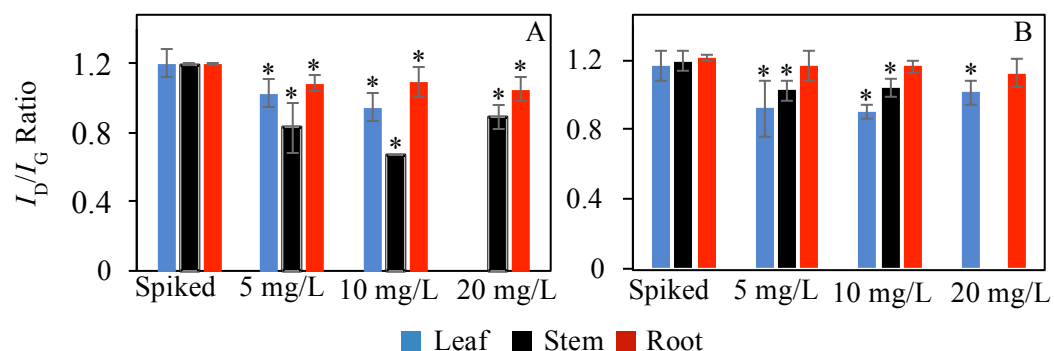


Figure S14. I_D/I_G ratios of p-MWCNT (A) and c-MWCNT (B) detected in the plants grown hydroponically with 5 mg/L, 10 mg/L or 20 mg/L of either MWCNT, in comparison with spiked plant tissues following the same HNO_3 digestion. MWCNT was not detected in the leaves of plants exposed to 20 mg/L p-MWCNT, nor in the stems of plants exposed to 20 mg/L c-MWCNT. Error bars represent the standard deviations of 3–10 measurements. Asterisk indicates a significant difference between MWCNTs in the hydroponic plant tissues and those in the spiked tissues.

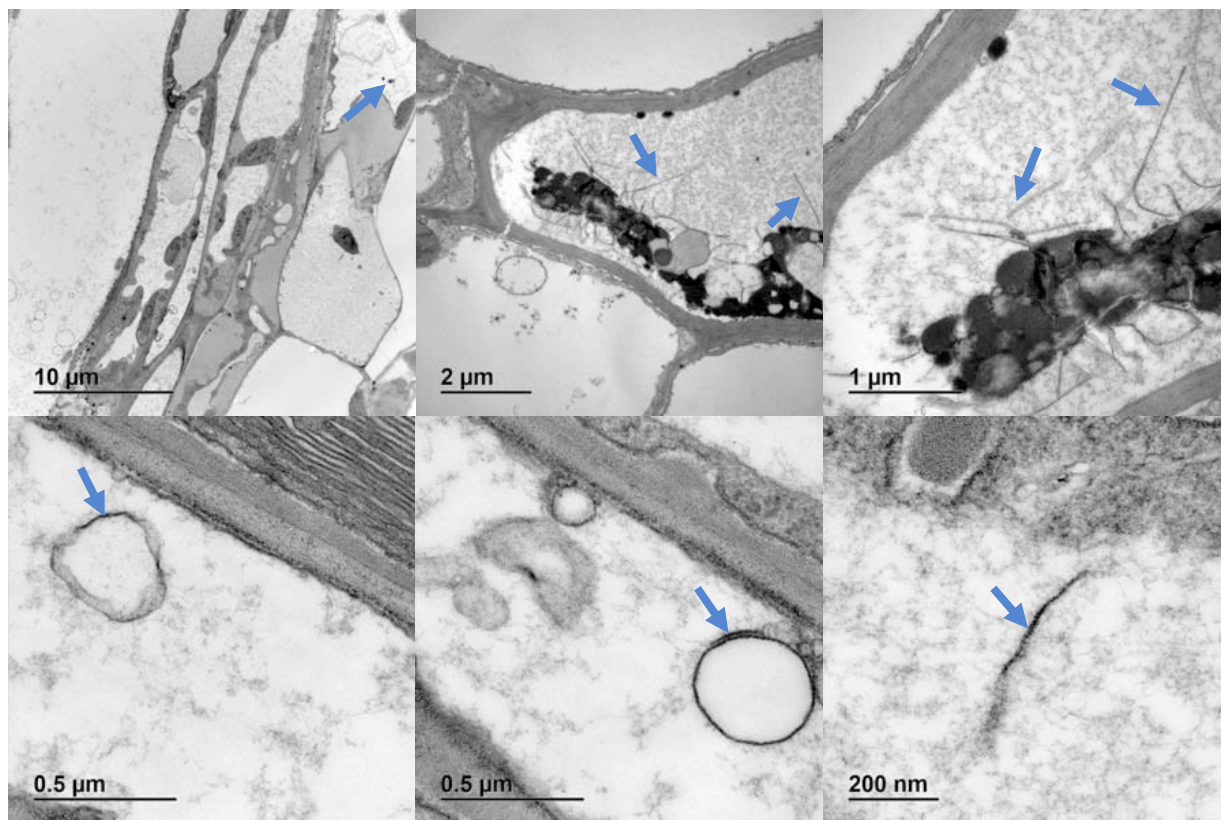


Figure S15. TEM images of MWCNTs in lettuce leaf cells. MWCNTs are indicated by blue arrows.

321 **Table S1. Physicochemical properties of MWCNTs used in this study.**¹²

Properties	p-MWCNT (as received)	p-MWCNT (sonicated)	c-MWCNT (as received)	c-MWCNT (sonicated)
Average diameter (nm) ^a	9.5	NA ^b	9.5	NA
Average length (μm) ^a	1.0	NA	1.0	NA
Carbon (%) ^a	>95.0	NA	>80.0	NA
COOH (%) ^a	NA	NA	<8.0	NA
Metal oxide (%) ^a	<5.0	NA	<5.0	NA
COOH (surface) (%) ^c	1.2	0.94	1.95	4.83
C=O (surface) ^c	4.28	4.56	5.07	0.97
C-O (surface) ^c	7.71	8.28	9.62	12.73
Amorphous carbon (%) ^d	1.77	3.87	5.50	4.22

322 ^aBased on the manufacturer (diameter and length determined using TEM; carbon purity, COOH
323 content, and metal oxide determined using thermal gravimetric analysis (TGA));

324 ^bNA, not available;

325 ^cDetermined by X-ray photoelectron spectroscopy analysis; percentages of COOH, C=O, C-O
326 groups were calculated from deconvolution of the C1s peaks;¹³⁻¹⁵

327 ^dEstimated by mass loss during decomposition at 500–550 °C in TGA.¹⁴

328

329 **References**

- 330 1. M. J. Karnovsky, *J. Cell. Biol.*, 1965, 27, A137-138.
- 331 2. M. A. Hayat, *Principles and Techniques of Electron Microscopy: Biological*
332 *Applications*, Cambridge University Press, 4th Edition, 2000.
- 333 3. C. M. Rico, S. Majumdar, M. Duarte-Gardea, J. R. Peralta-Videa and J. L. Gardea-
334 Torresdey, *J. Agric. Food Chem.*, 2011, 59, 3485-3498.
- 335 4. P. Miralles, T. L. Church and A. T. Harris, *Environ. Sci. Technol.*, 2012, 46, 9224-9239.
- 336 5. R. Nair, S. H. Varghese, B. G. Nair, T. Maekawa, Y. Yoshida and D. S. Kumar, *Plant*
337 *Sci.*, 2010, 179, 154-163.
- 338 6. X. Ma, J. Geiser-Lee, Y. Deng and A. Kolmakov, *Sci. Total Environ.*, 2010, 408, 3053-
339 3061.
- 340 7. G. Zhai, S. M. Gutowski, K. S. Walters, B. Yan and J. L. Schnoor, *Environ. Sci.*
341 *Technol.*, 2015, 49, 7380-7390.
- 342 8. J. E. Canãs, M. Long, S. Nations, R. Vadan, L. Dai, M. Luo, R. Ambikapathi, E. H. Lee
343 and D. Olszyk, *Environ. Toxicol. Chem.*, 2008, 27, 1922-1931.
- 344 9. P. Begum, R. Ikhtiari, B. Fugetsu, M. Matsuoka, T. Akasaka and F. Watari, *Appl. Surf.*
345 *Sci.*, 2012, 262, 120-124.
- 346 10. D. Lin and B. Xing, *Environmen. Pollut.*, 2007, 150, 243-250.
- 347 11. E. Katz and I. Willner, *Chemphyschem*, 2004, 5, 1085-1104.
- 348 12. Y. You, K. K. Das, H. Guo, C.-W. Chang, M. Navas-Moreno, J. W. Chan, P. Verburg, S.
349 R. Poulson, X. Wang, B. Xing and Y. Yang, *Environ. Sci. Technol.*, 2017, 51, 2068-2076.
- 350 13. M. Zhang, L. Shu, X. Shen, X. Guo, S. Tao, B. Xing and X. Wang, *Environ. Pollut.*,
351 2014, 195, 84-90.
- 352 14. V. Datsyuk, M. Kalyva, K. Papagelis, J. Parthenios, D. Tasis, A. Siokou, I. Kallitsis and
353 C. Galiotis, *Carbon*, 2008, 46, 833-840.
- 354 15. K. A. Wepasnick, B. A. Smith, J. L. Bitter and D. H. Fairbrother, *Anal. Bioanal. Chem.*,
355 2010, 396, 1003-1014.